Electromagnetic Biology and Medicine

ISSN: 1536-8378 (Print) 1536-8386 (Online) Journal homepage: www.tandfonline.com/journals/iebm20

In vitro stimulation with radiofrequency currents promotes proliferation and migration in human keratinocytes and fibroblasts

María Luisa Hernández-Bule, Elena Toledano-Macías, Aida Naranjo, Marina de Andrés-Zamora & Alejandro Úbeda

To cite this article: María Luisa Hernández-Bule, Elena Toledano-Macías, Aida Naranjo, Marina de Andrés-Zamora & Alejandro Úbeda (2021) In vitro stimulation with radiofrequency currents promotes proliferation and migration in human keratinocytes and fibroblasts, Electromagnetic Biology and Medicine, 40:3, 338-352, DOI: 10.1080/15368378.2021.1938113

To link to this article: https://doi.org/10.1080/15368378.2021.1938113

© 2021 The Author(s). Published with license by Taylor & Francis Group, LLC.

View supplementary material

Published online: 27 Jul 2021.

Submit your article to this journal

Article views: 4331

View related articles

View Crossmark data

Citing articles: 12 View citing articles

Full Terms & Conditions of access and use can be found at
https://www.tandfonline.com/action/journalInformation?journalCode=iebm20

ELECTROMAGNETIC BIOLOGY AND MEDICINE
2021, VOL. 40, NO. 3, 338–352
https://doi.org/10.1080/15368378.2021.1938113

Taylor & Francis
Taylor & Francis Group

OPEN ACCESS Check for updates

In vitro stimulation with radiofrequency currents promotes proliferation and migration in human keratinocytes and fibroblasts

María Luisa Hernández-Bule[a], Elena Toledano-Macías[a], Aida Naranjo[b], Marina de Andrés-Zamora[b], and Alejandro Úbeda[a]

[a]Servicio de Bioelectromagnetismo, Hospital Universitario Ramón y Cajal, IRYCIS, Madrid, Spain; [b]Departamento de Ingeniería Eléctrica, Escuela Técnica Superior de Ingeniería y Diseño Industrial, Universidad Politécnica de Madrid, Madrid, Spain

ABSTRACT

Capacitive-resistive electric transfer (CRET) therapies have been proposed as strategies for regeneration of cutaneous tissue lesions. Previous studies by our group have shown that intermittent stimulation with 448 kHz CRET currents at subthermal densities promotes in vitro proliferation of human stem cells involved in tissue regeneration. The present study investigates the effects of the in vitro exposure to these radiofrequency (RF) currents on the proliferation and migration of keratinocytes and fibroblasts, the main cell types involved in skin regeneration. The effects of the electric stimulation on cell proliferation and migration were studied through XTT and wound closure assays, respectively. The CRET effects on the expression and location of proteins involved in proliferation and migration were assessed by immunoblot and immunofluorescence. The obtained results reveal that electrostimulation promotes proliferation and/or migration in keratinocytes and fibroblasts. These effects would be mediated by changes observed in the expression and location of intercellular adhesion proteins such as β-catenin and E-cadherin, of proteins involved in cell-to-substrate adhesion such as vinculin, *p*-FAK and the metalloproteinase MMP-9, and of other proteins that control both processes: MAP kinases *p*-p38, *p*-JUNK and *p*-ERK1/2. These responses could represent a mechanism underlying the promotion of normotrophic wound regeneration induced by CRET. Indeed, electric stimulation would favor completion of granulation tissue formation prior to the closure of the outer tissue layers, thus preventing abnormal wound cicatrization or chronification.

ARTICLE HISTORY
Received 16 March 2021
Accepted 23 May 2021

KEYWORDS
Electrotherapy; skin regeneration; proliferation and migration proteins

Introduction

Fibroblast proliferation and migration are crucial processes in skin regeneration, and they allow for fibroplasia and synthesis of the extracellular matrix called granulation tissue, mainly composed of fibronectin, collagen and hyaluronic acid. In the subsequent re-epithelialization step, epidermal keratinocytes proliferate and migrate through the granulation tissue, covering the underlying tissue and leading to the process of tissue contraction, in which fibroblasts turn into myofibroblasts and close the wound by pulling in the edges of it (Stadelmann et al. 1998). When this highly ordered process is disrupted or retarded, chronic wounds are generated that usually consist of skin ulcerations associated with ischemia, prolonged inflammation, pressure necrosis, infections or tumors. For the affected patient, these injuries entail high economic costs and considerable disturbance of his/her life quality. In recent years, treatments traditionally applied to these injuries, including wound care and dressings, skin substitutes, negative pressure wound therapy, growth factors or hyperbaric oxygen administration (Han and Ceilley 2017), have been reinforced by the use of electric or electromagnetic therapies, driven by new evidence on the effects of endogenous or exogenous electrical currents on skin regeneration. For instance, it has been reported that the use of electric stimulation as an adjuvant therapy can accelerate and improve closure of pressure ulcers in patients having spinal cord injuries (Houghton et al. 2010; Lala et al. 2016) or chronic ulcerations (Barnes et al. 2014). In rats submitted to surgical incision, treatment with extremely low frequency (ELF) pulsed currents increased the number of blood vessels in the wound region, as well as the amount of fibroblasts and collagen fibers present in the area (Borba et al. 2011). At the cellular level, static or low-frequency electric fields and currents are capable of acting on various processes involved in wound

CONTACT María Luisa Hernández-Bule mluisa.hernandez@hrc.es; mhbule@salud.madrid.org Servicio de Bioelectromagnetismo. Hospital Universitario Ramón y Cajal, IRYCIS. Ctra. Colmenar Viejo km 9.100, 28034, Madrid, Spain,Telephone: 34-91-3368699
Supplemental data for this article can be accessed on the publisher's website.

© 2021 The Author(s). Published with license by Taylor & Francis Group, LLC.
This is an Open Access article distributed under the terms of the Creative Commons Attribution-NonCommercial-NoDerivatives License (http://creativecommons.org/licenses/by-nc-nd/4.0/), which permits non-commercial re-use, distribution, and reproduction in any medium, provided the original work is properly cited, and is not altered, transformed, or built upon in any way.

regeneration, including promotion of dermal fibroblast proliferation and migration, myofibroblastic transdifferentiation or increased secretion of growth factors (Rouabhia et al. 2013; Tai et al. 2018), as well as promotion of collective migration of epithelial cells (Li et al. 2012).

The application of intermediate frequency and radiofrequency (RF) electric therapies has also proven effective in the treatment of venous or chronic pressure ulcers (Conner-Kerr and Isenberg 2012; Fletcher 2011) or wounds in diabetic patients (Frykberg et al. 2011). Likewise, in surgically injured diabetic mice, RF exposure induced accelerated closure of the skin incision by promoting proliferation of dermal cells (Li et al. 2011), acceleration of neocollagenogenesis and neoangiogenesis and increase of dermal thickness (Meyer et al. 2017). At the cellular level, in vitro exposure to pulsed RF currents has been reported to increase cell proliferation and collagenogenesis in fibroblasts (Kao et al. 2013).

Also within the RF spectrum, non-invasive capacitive-resistive electric transfer (CRET) therapies apply 448–600 kHz electric currents in order to induce hyperthermia in target tissues, the thermal increase being a function of various physical and physiological parameters, including the specific impedance of the exposed tissue (Kotnik and Miklavcic 2000; Grimnes and Martinsen 2000). CRET therapies have been used successfully in regeneration of muscle (Takahashi et al. 1999), bones (Kumaran and Watson 2019), tendons and ligaments (Bito et al. 2019) and skin (Naranjo et al. 2020). The block of in vitro experimental data has provided evidence that the regenerative effects of these therapies could be mediated by stimulation of stem cell proliferation through activation of proteins involved in cell cycle regulation (Hernandez-Bule et al. 2014a) or by promotion of early chondrocyte differentiation through increased synthesis of cartilage-specific extracellular matrix molecules, such as collagen and glycosaminoglycans (Hernandez-Bule et al. 2017). With regard specifically to wound healing and skin regeneration, CRET treatment has been reported to induce expression of fibroblast growth factor 2 and promote neocollagenesis and neoangiogenesis in the tissue (Meyer et al. 2017).

However, in the lack of sufficient experimental evidence, the current knowledge on the cellular and molecular mechanisms underlying the effects of CRET-type electric therapies operating in a frequency range below 1 MHz, is still rather limited. Substantial expansion of such knowledge is essential to optimize the applications of these physical treatments in wound regeneration. The present study investigates the effects of in vitro exposure to CRET electric currents on cell types and cellular processes involved in skin regeneration. To this end, relevant aspects of the proliferation and migration of human fibroblasts and keratinocytes exposed to 448 kHz currents applied at subthermal densities have been analyzed. The obtained results indicate that the reported CRET effects on skin regeneration promotion could be exerted, at least in part, through induction of keratinocyte and fibroblast proliferation and/or migration mediated by changes in the expression and location of a number of cell-to-cell and cell-to-substrate adhesion proteins.

Material and methods

Cell culture

Two cell types were used: human dermal fibroblasts (HF) isolated from neonatal foreskin (cat. no. C-004-5 C, Thermo Fisher, Carlsbad, CA, USA) and human epidermal keratinocytes HaCaT (CLS Cell Lines Service, 300493, Heidelberg, Germany). Both cell types were seeded in medium composed of high-glucose D-MEM (Biowhittaker, Lonza, Verviers, Belgium) supplemented with 10% inactivated foetal bovine serum (Gibco, MA USA), 1% glutamine and 1% penicillin-streptomycin (Gibco) and maintained in a 5% CO_2 atmosphere at a temperature of 37°C inside CO_2 incubators (Thermo Fisher Scientific, Waltham, MA, USA).

The cells were subcultured once a week and plated on the bottom of 60 mm Petri dishes (Nunc, Roskilde, Denmark), except for immunofluorescence assays, in which the cells were seeded on glass coverslips placed on the bottom of the plates. Depending on the aim of the corresponding experiment, a total of 8 or 10 Petri dishes were used per experimental replicate. Both cell lines were periodically tested for mycoplasma.

Electric treatment

The procedure for RF exposure has been described in detail elsewhere (Hernandez-Bule et al. 2014b, 2007). Briefly, 3 or 4 days after seeding, depending on the experiment, pairs of sterile stainless steel electrodes designed ad hoc for in vitro stimulation were inserted in all Petri dishes and connected in series. Only the electrodes corresponding to plates intended for electrical stimulation were energized using a signal generator (Indiba Activ HCR 902, INDIBA®, Barcelona, Spain), while the remaining plates were sham-exposed simultaneously inside an identical, separate CO_2 incubator. The intermittent stimulation pattern consisted of 5-minute pulses of 448 kHz, sine wave current delivered at subthermal densities of 50 or 100 μA/mm^2 (Figure S1), separated by 4-hour interpulse lapses and administered

for a total of 6 h, 12 h or 48 h (Figure S2). Such exposure parameters have been shown to stimulate the proliferation and early differentiation of human, adipose-derived stem cells (Hernandez-Bule et al. 2016, 2014a, 2017).

XTT proliferation assay

Cell proliferation was determined by XTT assay (Roche, Switzerland). The HaCaT and HF cultures were seeded at densities of 4500 cells/cm^2 and 5500 cells/cm^2, respectively, and incubated for 3 days. After 48 h of CRET- or sham-treatment, the cells were incubated for 3 hours with the tetrazolium salt XTT in a 37°C and 6.5% CO_2 atmosphere, as recommended by the manufacturer. The metabolically active cells reduced XTT into coloured formazan compounds that were quantified with a microplate reader (TECAN, Männedorf, Switzerland) at a 492 nm wavelength. At least 3 experimental replicates per cell type were conducted.

Wound assay

In each experimental replicate of the wound closure assay, HF (31000 cells/cm^2) or HaCaT (6800 cells/cm^2) were seeded on 8 plates and incubated at 37°C until confluence: at 24 h (HF) or 4 days (HaCaT) post-plating. Then, using a plastic pipette tip, a wound was scratched on the confluent monolayer of each of the plates. Dishes were washed with PBS (Gibco) to eliminate debris, and the cultures were maintained in high-glucose D-MEM medium supplemented with 10% inactivated foetal bovine serum (Gibco), 1% glutamine and 1% penicillin-streptomycin (Gibco). Next, 4 plates were exposed to CRET for 6 or 12 hours, while the remaining plates were sham-exposed for the same intervals. At 0, 6 and 12 h after scratching, micrographs were taken of 3 equidistant points in the wounds, using a digital camera (Nikon DS-Ri2) coupled to an inverted microscope (Nikon Eclipse Ts2R). The wound closure rate was determined by dual analysis of the obtained images, using two different software: a) standard Photoshop software (Adobe Photoshop CS3, Extended version 10.0), and b) Matlab-based (Mathworks) computer tools named Image Segmentation for Quantitative Assessment of Cell Migration (ISAM), developed ad hoc for quantitative assessment of the gap area, as described below.

Image segmentation for quantitative assessment of cell migration

Cell migration was assessed by studying the wound closure evolution through computational analysis of the micrographs. For this purpose, two ISAM applications, one for each of the studied cell types, were implemented using the Matlab Development Environment. Briefly, the first application processes the HF images to determine the wound area (Figure S3). This application equalizes the histogram of the image's red component to increment the contrast between gray tone levels. Next, the algorithm applies the canny operator to detect the wound edges in the image, which then passes through different morphological operations including dilatation, geodesic opening and erosion, to isolate the wound as the only object in the image. Finally, the algorithm white marks the wound edges, counts the pixel number within the wound area and calculates the corresponding surface out of the whole image. The second application similarly processes the wound images of HaCaT cultures to determine and quantify the gap area.

Immunofluorescence assay for expression of cell adhesion proteins vinculin, p-FAK, β-catenin and E-cadherin

The HaCaT keratinocyte cultures were seeded at a density of 13600 cells/cm^2. These cells migrate collectively, and the cellular distribution of adhesion proteins during migration differs depending on whether the cells are located on the wound's front (leader cells) or on the monolayer (follower cells); see (Mayor and Etienne-Manneville 2016) for a review. Thus, in order to study both distribution patterns, on day four post-seeding on coverslips, when high confluence was reached, a wound on the HaCaT monolayer was scratched before the stimulation onset. In contrast, fibroblast do not migrate collectively, so they were seeded at a density of 28000 cells/cm^2 and the electric stimulation started 24 hours afterwards. As at this interval the HF cultures had not yet reached high confluence, the study of the CRET effects on proteins involved in the type of individual migration characteristic of these cells, could be carried out with no need of scratching a wound.

After 6 or 12 hours of RF- or sham-exposure, the samples were fixed with 4% paraformaldehyde (Merk, Darmstadt, Germany) and incubated overnight at 4°C with anti-vinculin monoclonal antibody (1:800; cat. no. V9131; Sigma Aldrich, Israel), anti-*p*-FAK monoclonal antibody (1:50; cat. no. 611722; BD Biosciences; CA, USA), anti-β-catenin monoclonal antibody (1:100, cat. no. SC-7963; Santa Cruz Biotechnology, TX, USA) and anti E-cadherin monoclonal antibody (1:50, cat. no. 610182; Santa Cruz Biotechnology). Afterwards, the samples were fluorescence stained with Alexa Fluor™ 568 goat anti-mouse IgG (1:500; cat. no. A11031; Invitrogen, USA) for 1 h at room temperature and the cell nuclei were counterstained with

bisBenzimide H33258 trihydrochlorid (Sigma, MO, USA). Photomicrographs were taken of the monolayers in both cell types and of the wound in HaCaT, and the images were computer analyzed using an inverted fluorescence microscope (Nikon Eclipse Ts2R) coupled to a digital camera (Nikon DS-Ri2) and Computer-Assisted Image Analysis software (Analy-SIS, GMBH, Munich, Germany). At least three replicates of each experiment were performed per protein, exposure time and cell type.

Immunoblot for vinculin, p-FAK, β-catenin, E-cadherin, MMP-9, p-ERK1/2, p-p38 and p-JUNK

HF (31000 cells/cm^2) and HaCaT (6800 cell/cm^2) were plated in 8 dishes and incubated at 37°C until confluence, at 24 h (HF) or day 4th (HaCaT) post seeding. Cultures were RF- or sham-exposed and the cells were lysed for protein extraction at 6 or 12 hours from the exposure onset. The immunoblot procedure has been described in detail elsewhere (Hernandez-Bule et al. 2007, 2017). Briefly, the protein samples (100 µg protein aliquots) were separated in 10% sodium dodecyl sulphate-polyacrylamide gel and electrophoretically transferred to nitrocellulose membrane (Amersham, Buckinghamshire, UK). Blots were incubated at 4°C overnight in anti-vinculin monoclonal antibody (1:400, cat. no. V9131, Sigma Aldrich), anti-*p*-FAK monoclonal antibody (1:1000; cat. no. 611722; BD Biosciences), anti-β-catenin monoclonal antibody (1:200, cat. no. SC-7963; Santa Cruz Biotechnology), anti-E-cadherin monoclonal antibody (1:20000, cat. no. 610182; BD Biosciences), anti-MMP-9 monoclonal antibody (1:1000, cat. no. AB76003; Abcam, UK), anti-*p*-ERK1/2 polyclonal antibody (1:1000; cat. no.44680 G; Invitrogen Bioservice, India), anti-*p*-p38 monoclonal antibody (1:2000, cat. no. #9216; Cell signaling, MA, USA) and anti-*p*-JUNK monoclonal antibody (1:1000, cat. no. #4668; Cell signaling). Anti-β-actin monoclonal antibody (1:5000, cat. no. A5441; Sigma-Aldrich) or GAPDH (1:500, cat. no. sc-25778; Santa Cruz Biotechnology) were used as loading controls. The membranes were incubated for one hour at room temperature with anti-rabbit IgG conjugated to IRdye 800 CW (1:10000, cat. no. 926–32211; LI-COR Biosciences, Nebraska, USA) and with anti-mouse IgG conjugated to IRdye 680 LT (1:15000, cat. no. 926–68020; LI-COR Biosciences). Then, the membranes were scanned with a LI-COR Odyssey scanner (LI-COR Biosciences). The obtained bands were densitometry evaluated (PDI Quantity One 4.5.2 software, BioRad). At least 5 experimental replicates were conducted per protein and cell type. All values were normalized over the loading control. No immunofluorescence analysis was conducted for MAPKs or MMP-9, given the scarce potential relevance of any changes that might occur in their intracellular location.

Statistical analysis

All procedures and analyses were conducted in blind conditions for treatment. At least three independent replicates were conducted per experiment, cell type, current density or exposure interval, the results being expressed as means ± standard deviation (SD) or standard error of the mean (SEM). Unpaired Student's t-test was applied using GraphPad Prism 6.01 software (GraphPad Software, San Diego, CA, USA). Differences $p < 0.05$ were considered significant statistically.

Results

CRET effects on cell proliferation

The results of the XTT assay for cell proliferation depicted in Figure 1 revealed that a 48-hour intermittent exposure to the subthermal current density of 50 µA/mm^2 did not change significantly proliferation in keratinocytes or neonatal fibroblasts, whereas treatment with 100 µA/mm^2 significantly increased proliferation in both cell types (Figure 1). On the basis of these results, in subsequent experimental tests only the current density of 100 µA/mm^2 was applied.

CRET effects on cell migration

Wound closure

The results from dual image analysis on HaCaT keratinocytes, summarized in Figure 2, revealed that at 6 h from the exposure onset (two CRET pulses of 5 min, at t = 0 h and t = 4 h) the cultures showed retarded wound closure rate. The differences with respect to controls were statistically significant when the standard software was applied, but not when the data were analyzed with the ISAM software we developed. By contrast, in the HF cultures exposed for 6 hours, wound closure was significantly accelerated with respect to their sham-exposed controls, as revealed by both software. At 12 hours, the wound closure was complete in the vast majority of cultures of both cell types, and no significant differences in closure rates could be detected between the CRET-exposed cultures and their controls.

The orientation or alignment of the cells with respect to the RF current was routinely analyzed. Image analysis revealed no signs of alignment in the monolayer zone or

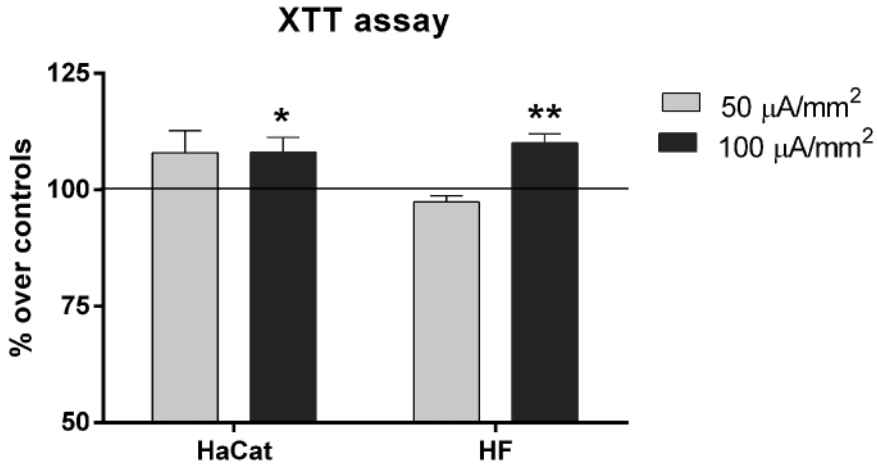


Figure 1. XTT assay. Cell proliferation after 48 h of intermittent CRET exposure at current densities of 50 or 100 μA/mm^2. Data are means ± SEM normalized over the corresponding sham-exposed controls represented by the reference line 100%. Between 3 and 7 experimental replicates per cell type. *: 0.05 > p ≥ 0.01; **: 0.01 > p ≥ 0.001; Student´s t-test.

in the migration front in either cell type (data not shown).

Cell-to-substrate adhesion proteins

Vinculin and focal adhesion kinase *p*-FAK are part of the adhesion complexes and lamellipodia that form and degrade during cell migration (Thievessen et al. 2015). The chronology of the changes in the expression and intracellular location of both proteins was analyzed by immunofluorescence and immunoblot.

Vinculin. In keratinocytes, CRET induced vinculin overexpression, both at 6 and 12 hours of treatment (Figure 3) and did not change significantly the location of the vinculin labeling after 6 hours of treatment: in both control and treated samples, the labeling was diffuse and located at the cytoplasm of keratinocytes in the monolayer, whereas in the cells located on the wound edges, vinculin formed plaques in the migration front (Figure 4). At 12 hours, when wound closure was complete, vinculin maintained its preferentially cytoplasmic distribution in control samples, whereas in CRET-treated cultures the protein had moved to the cell membrane, concentrating at junctions of focal adhesion to the substrate, where the protein is functionally active.

In fibroblasts, CRET induced significant reduction with respect to controls in the expression of vinculin after 6 hours of electric stimulation, but not after 12 hours of treatment (Figure 3). In these cells, which unlike keratinocytes, do not migrate forming well defined fronts, the vinculin labeling formed plaques located on the plasma membrane, both in samples treated for 6 hours and in their controls. At 12 hours, the treated samples maintained the labeling at their membrane location, while in control cells it had moved to the cytoplasm (Figure 5).

P-FAK. In keratinocytes, CRET induced statistically significant overexpression of *p*-FAK after 6 hours, but not after 12 hours of treatment (Figure 3). Regarding location, at 6 hours the sham-exposed keratinocytes present in the monolayer showed only diffuse cytoplasmic *p*-FAK labeling, whereas those treated with CRET also had nuclear marking (Figure 4). As for keratinocytes located on the migratory front, in those sham-exposed for 6 h the labeling showed the diffuse morphology and cytoplasmic location described above, while in those treated with CRET, *p*-FAK preferentially displayed a nuclear location. At 12 hours, when the wound closure was complete, the control samples preferentially showed a cytoplasmic marking, while in those treated with CRET, *p*-FAK displayed a dotted and diffused nuclear distribution (Figure 4).

In fibroblasts, CRET induced significant reduction of p-FAK expression after 6 hours of treatment, and overexpression at the end of the 12 hour treatment (Figure 3). As for p-FAK labeling, at 6 hours it was very scarce, diffuse and preferentially distributed in the cytoplasm of controls, whereas treated cells showed additional labeling located at the plasma membrane level. At 12 hours, the marking was exclusively cytoplasmic, with no significant differences between the electrically stimulated samples and their controls (Figure 5).

Cell-to-cell adhesion proteins

β-catenin. In keratinocytes, CRET significantly reduced the expression of β-catenin at the end of the first 6 hours of exposure but not after additional 6 hour treatment

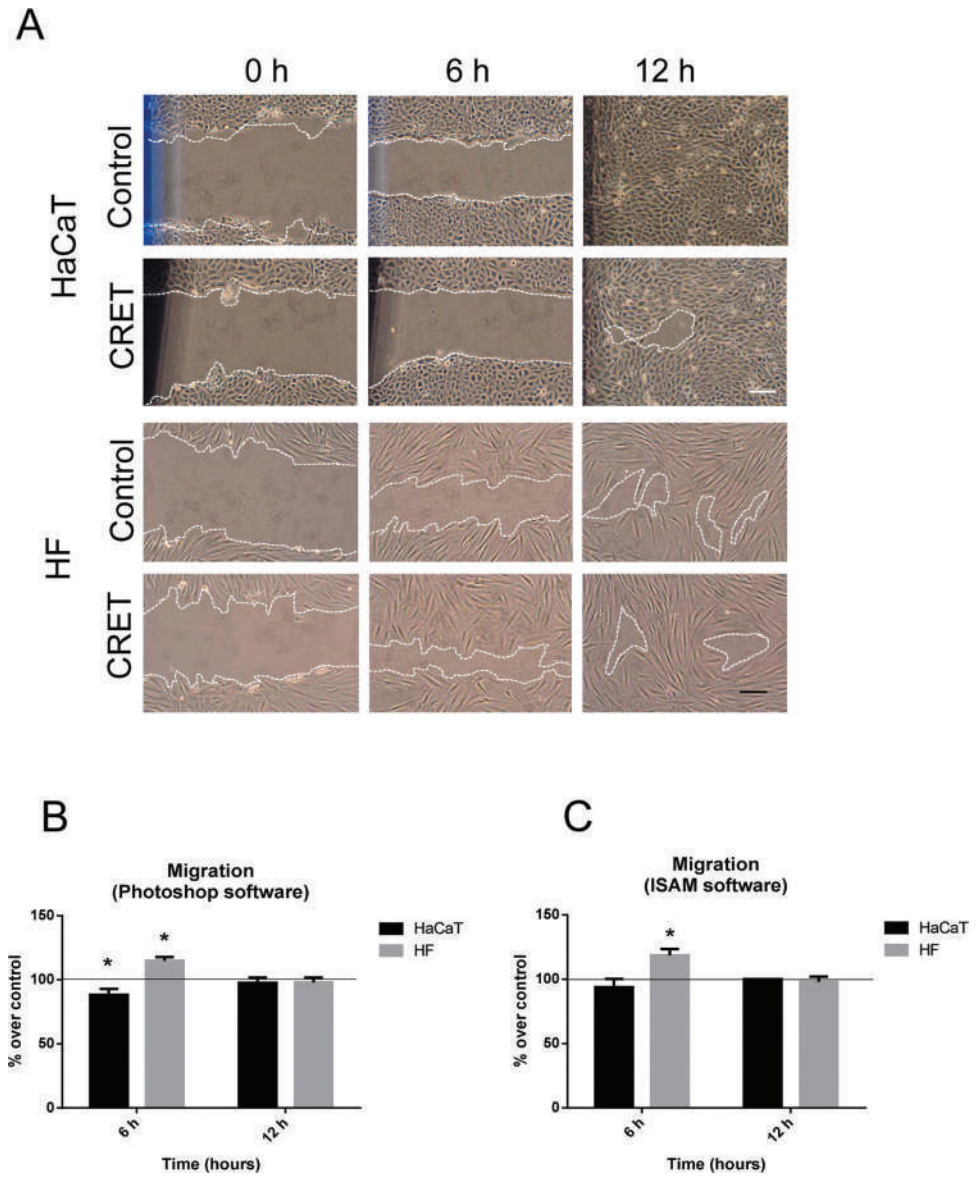


Figure 2. Wound Assay. A. Representative micrographs of the wound at t = 0 h, 6 h or 12 h from CRET- or sham-stimulation (Control) onset. Bars: 50 µm. The dotted white lines indicate the wound's edges. **B**. Computational quantification of the gap closure calculated as the mean distance (µm) between the edges in three equidistant points of the gap, using Photoshop software. **C**. Quantification of the area (μm^2) between the wound edges using ISAM software. Data de are means ± SD, normalized over the corresponding controls, represented by the reference line 100%, of six experimental replicates per cell type and time interval. *: $0.05 > p \geq 0.01$; Student´s t-test.

(Figure 3). At that time, control samples in the monolayer showed β-catenin labeling at the intercellular junctions, whereas the treated cells additionally showed diffuse cytoplasmic labeling. At the wound edges, the labeling in control cells was detected at the plasma membrane level in zones contacting with adjacent cells, but not in those next to the migration front. In treated cells the labeling was weaker and more diffuse than that in controls, and it was very scarce in the vicinity of plasma membranes adjacent to other cells. At 12 hours, the treated samples and their controls showed labeling patterns analogous to those observed at 6 hours (Figure 6).

In fibroblasts, 6 h of CRET treatment induced statistically significant overexpression of β-catenin, while after an additional 6 hour exposure, the expression of β-catenin was significantly reduced with respect to controls (Figure 3). In this cell type, which in culture shows little intercellular junctions, β-catenin formed scattered plaques located

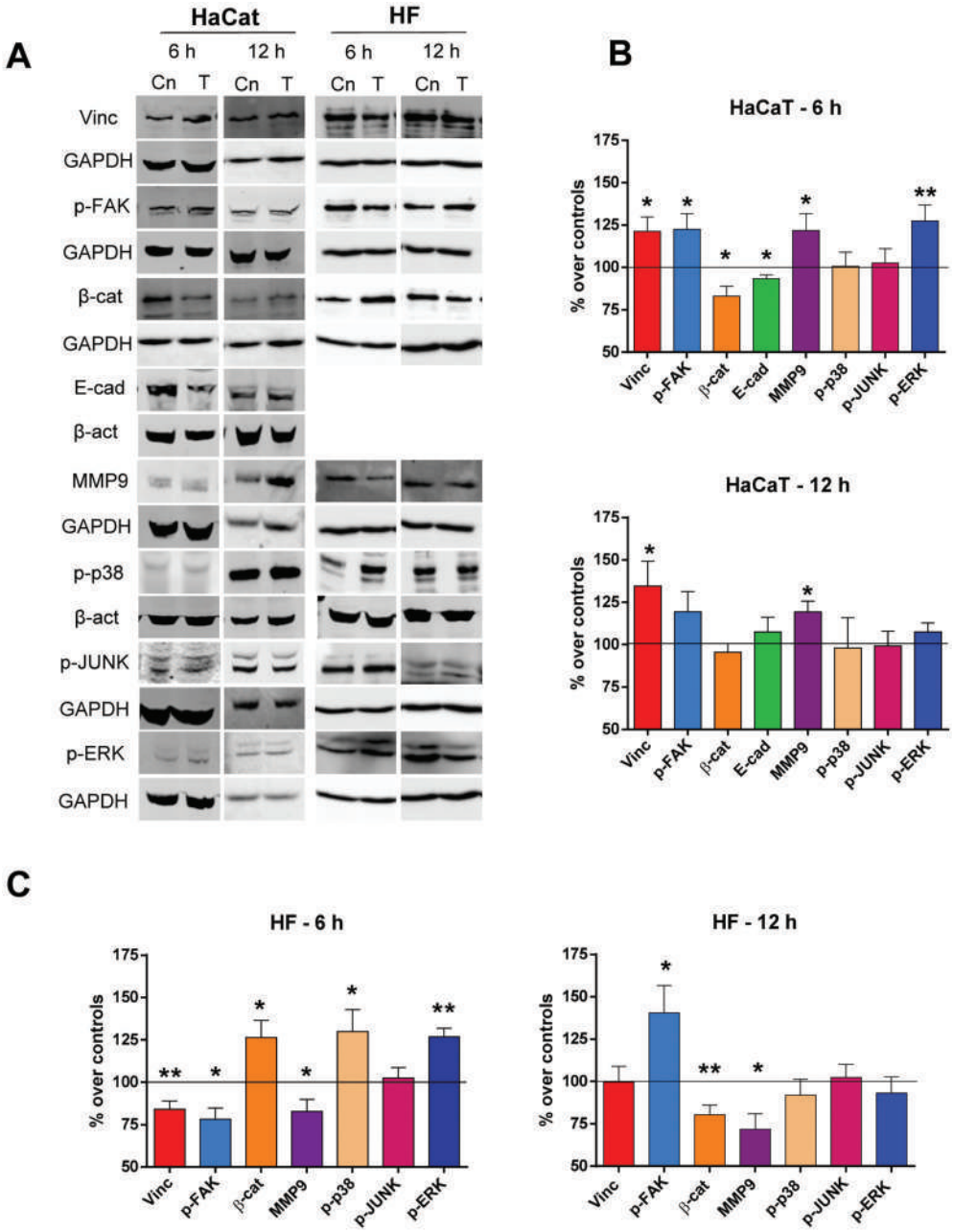


Figure 3. Immunoblot for protein expression. A. Representative blots at 6 h or 12 h of CRET or sham treatment (100 µg protein/lane). β-actin or GAPDH were used as loading control. Cn: Control. T: CRET treatment. **B**. Densitometry values for protein expression at 6 h or 12 h of CRET or sham treatment in keratinocytes HaCaT. **C**. Densitometry for protein expression at 6 h or 12 h of CRET or sham treatment in fibroblasts (HF). Data, normalized over the corresponding sham-exposed controls represented by the reference line 100%, are means ± SD of the protein/β-actin or protein/GAPDH ratios of at least 5 experimental repeats per protein and time interval. *: $0.05 > p \geq 0.01$; **: $0.01 > p \geq 0.001$; Student´s t-test.

near the membrane of some cells. CRET treatment for 6 or 12 hours induced no detectable changes with respect to controls in the labeling distribution or intensity (Figure 6).

E-cadherin. Since fibroblast were found not to express E-cadherin, the CRET effects on the expression and distribution of this protein were studied in keratinocytes only. In the treated samples, the expression of E-cadherin was found to be decreased relative to controls after 6 hours of exposure, but not after 12 hours (Figure 3). In addition, the 6-hour control cells located in the monolayer showed intense labeling, both at the plasma membrane level, in the vicinity of the intercellular junctions, as well as in dotted structures in the perinuclear region (Figure 6). In the

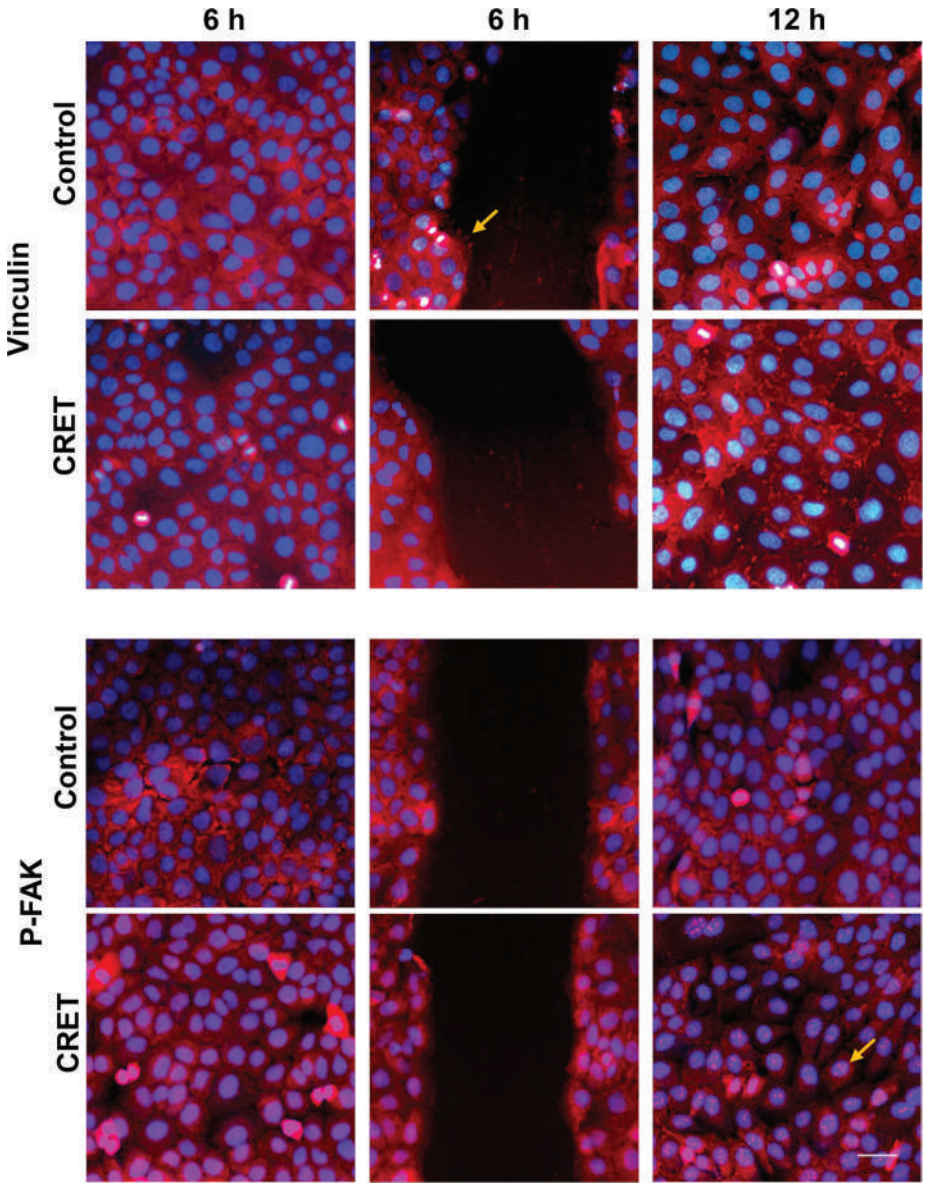


Figure 4. Immunofluorescence expression of Vinculin and *p*-FAK in keratinocytes. Monolayers (side columns) at 6 and 12 hours of CRET or sham treatment (Control), and in wound edges (central column) at 6 hours only. Representative merged micrographs. Red: vinculin or *p*-FAK labeling. Blue: nuclei. Bar: 20 µm. Brightness and contrast adjustments were applied to the whole of each image using Photoshop software. The adjustments in the micrographs of the treated samples were the same as those in the images of their controls. The arrows highlight presence of vinculin labeling on the membrane of 6-hour control cells located at the migration front, and that of *p*-FAK in the nuclei of 12-hour exposed cells.

corresponding treated cells, the E-cadherin labeling had disappeared from the intercellular junctions and no longer formed a continuous perimeter between adjacent cells. In the gap region of the 6-hour control samples, E-cadherin was present in the form of dotted or diffuse cytoplasmic labeling located in intercellular regions only, at the level of plasma membrane sections adjacent to other cells, but not at the migration front. In the corresponding exposed cells, E-cadherin had disappeared from the vicinity of the plasma membrane, becoming a stippled labeling located at the perinuclear region. After 12 hours of sham-treatment, the control samples showed intense labeling restricted to the immediate vicinity of the plasma membrane. By contrast, the treated samples showed diffuse, cytoplasmic labeling, though some plates were also detected at the plasma membrane level (Figure 6).

Other proteins involved in cell migration and proliferation

Metalloproteinase-9. In keratinocytes, MMP-9 mediates intercellular junction breakdown and cell

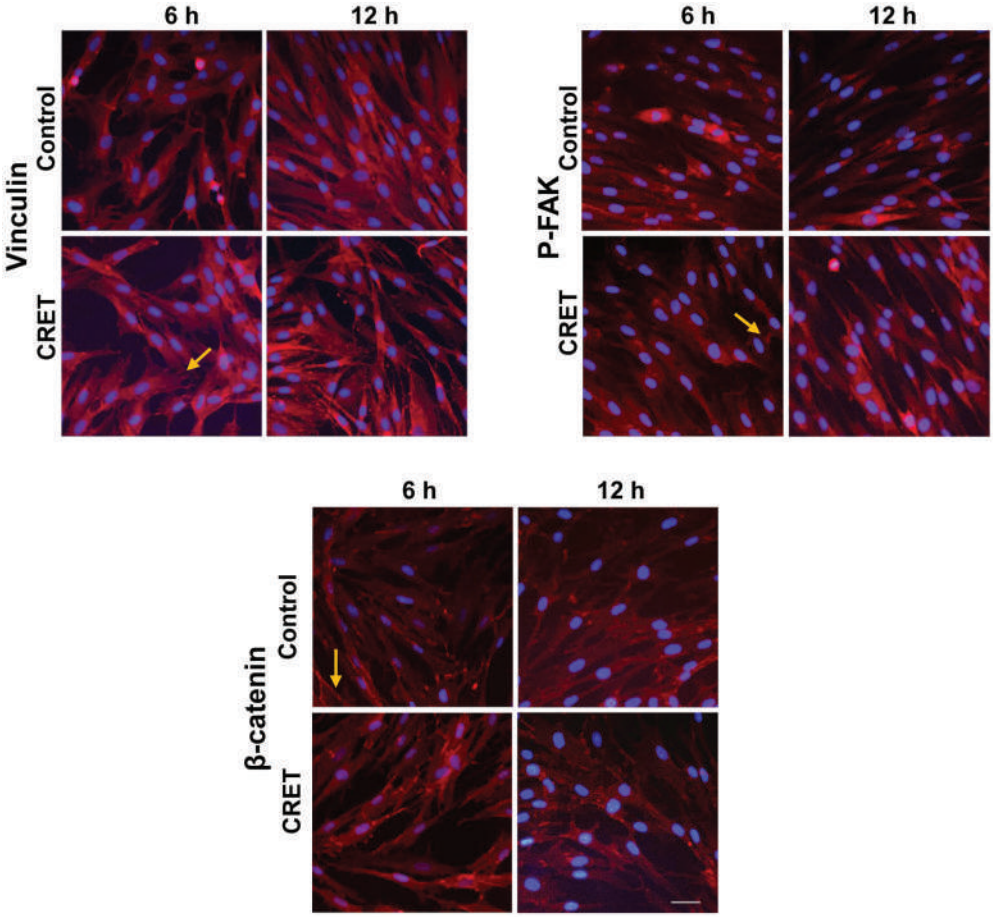


Figure 5. Immunofluorescence expression of Vinculin, *p*-FAK and β-catenin in fibroblasts. Monolayers at 6 or 12 hours of CRET or sham treatment (Control). Representative merged micrographs. Red: β-catenin, vinculin or *p*-FAK labeling. Blue: cell nuclei. Bar: 20 μm. Brightness and contrast adjustments were applied to the whole of each image using Photoshop software. The adjustments in the micrographs of the treated samples were the same as those in the images of their controls. Arrows show vinculin plaques and *p*-FAK and β-catenin labeling on the plasma membrane.

migration through its action on β-catenin. The immunoblot assay revealed statistically significant MMP-9 overexpression in keratinocyte cultures, both at 6 or 12 hours of treatment. By contrast, the expression of this metalloproteinase was significantly reduced in fibroblasts exposed to CRET for 6 or 12 hours (Figure 3).

MAPKs. The MAPK pathway proteins *p*-p38, *p*-JUNK and *p*-ERK1/2, are involved in cell migration and proliferation. In keratinocytes, *p*-p38 and *p*-JUNK expressions did not change significantly with respect to controls after 6 or 12 hours of treatment. In contrast, *p*-ERK1/2 overexpression was observed after 6 or 12 hours of electric exposure, although only for the 6-hour treatment the differences with respect to controls were statistically significant. In fibroblasts, CRET induced significant overexpression of *p*-p38 and *p*-ERK1/2 after 6 hours of exposure, but not after 12 hours. The expression of *p*-JUNK in HF was unaffected after 6 h or 12 h of treatment (Figure 3).

Discussion

There is growing interest in injury chronification prevention through the development of strategies aimed at promoting fast and efficient repair of wounds affecting the skin and underlying tissues. One of these strategies is based on the application of electric currents or electromagnetic fields for torpid wound treatment (Barnes et al. 2014). The present study investigates the cellular response to the exposure to RF electric currents that have been shown effective in skin lesion repair (Conner-Kerr and Isenberg 2012; Fletcher 2011; Frykberg et al. 2011). To this end, the effects of in vitro exposure to subthermal CRET currents on proliferation and migration of skin fibroblasts and keratinocytes have been analyzed. Previous studies by our group have shown

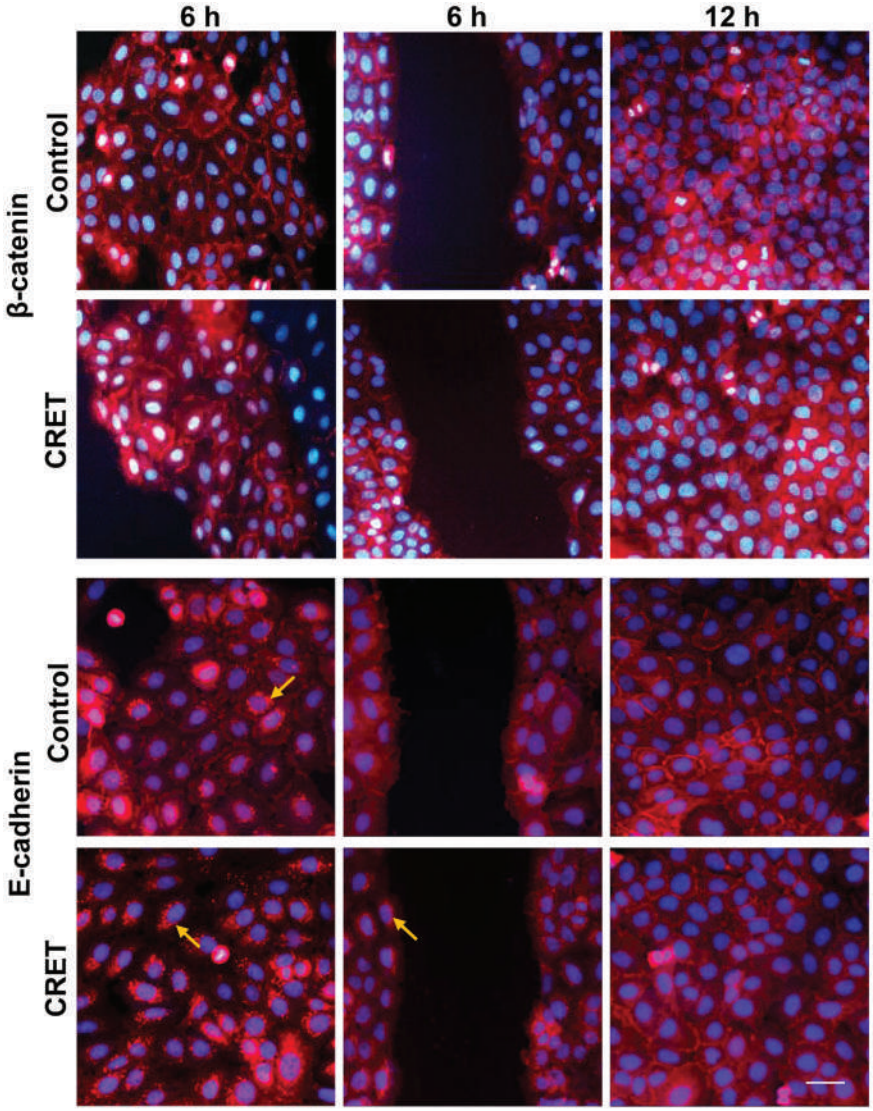


Figure 6. Immunofluorescence expression of β-catenin and E-cadherin in keratinocytes. Monolayers (side columns) at 6 h or 12 h of CRET or sham treatment (Control), and on the gap edges (central column) at 6 h. Representative merged images. Red: β-catenin and E-cadherin labeling. Blue: nuclei. Bar: 20 μm. Brightness and contrast adjustments were applied to the whole of each image using Photoshop software. The adjustments in the micrographs of the treated samples were identical to those in their controls. Arrows show dotted labeling of E-Cadherin at perinuclear locations.

that subthermal exposure to CRET currents promotes proliferation of human stem cells (Hernandez-Bule et al. 2014a) that are directly involved in neovascularization and wound regeneration (Kanji and Das 2017). The results reported in the present study show that CRET electrostimulation can also promote human fibroblast and keratinocyte proliferation, which suggests that the electrically induced proliferation of these three cell types could be involved in the regenerative effects attributed to CRET therapies.

In addition to proliferation, the tissue regeneration process requires cell migration in virtually all its phases. In order to initiate migration, the cell has to reorganize its cytoskeleton and dismantle adhesion complexes such as the desmosomes and adherens junctions that bind adjacent cells, as well as the hemidesmosomes and focal adhesions that attach the cell to its substrate. Next, the cell proceeds by emitting lamellipodia or filopodia (Santoro and Gaudino 2005), which in the type of collective migration typical of keratinocytes, only occurs in cells leading the migration front (Mayor and Etienne-Manneville 2016). The present study investigates the potential effects of the electric stimulation on proteins that are part of the aforementioned structures, whose expression and/or location undergo significant changes during cell migration. To our knowledge, no previous study has investigated the mechanisms underlying the dual proliferative and migratory response of the two

major types of human epithelial cells to subthermal stimulation with RF CRET currents.

Vinculin is a protein involved in cell-to-substrate adhesion and cell migration at the three-dimensional level. This anchorage to the substrate is the supporting point for the elongation, orientation and traction of the cytoskeleton during migration (Thievessen et al. 2015). Vinculin is mainly located in: 1) focal complexes present in the lamellipodia emitted by the cells situated on the migration front, and 2) focal adhesions present in the region of the plasma membrane that contacts with the substrate, connecting integrins with the cytoskeleton and attaching the cell to the substrate. In order to be functionally active, vinculin must be located in cytoplasm regions close to the plasma membrane, although prior to migration, unfastening and degradation of this protein are also necessary for disruption of the cell-to-substrate junction (Goldmann 2016). In keratinocytes, the CRET-induced increase in the expression and translocation of vinculin to the membrane of cells placed on the migration front (Figures 7 and Figures 8) could be expected to promote cell migration. However, the wound assay did not detect increased migration rates in electrically treated keratinocytes.

In fibroblasts, the wound assay shows that electric stimulation had significantly promoted cell migration on the first 6 hours of treatment. The immunoblot assay for the same time interval revealed significant reduction of vinculin expression, which could indicate that the phase of protein unfastening and degradation preceding cell migration was occurring at that very time. At 12 hours, the gap was virtually closed, both in the exposed samples and in their controls. However, while in control fibroblasts vinculin mainly showed the disperse cytoplasmic location characteristic of functional inactivity, in the RF exposed samples the protein appeared in the vicinity of the plasma membrane, a typical location in migrating cells (Figures 7 and Figures 8).

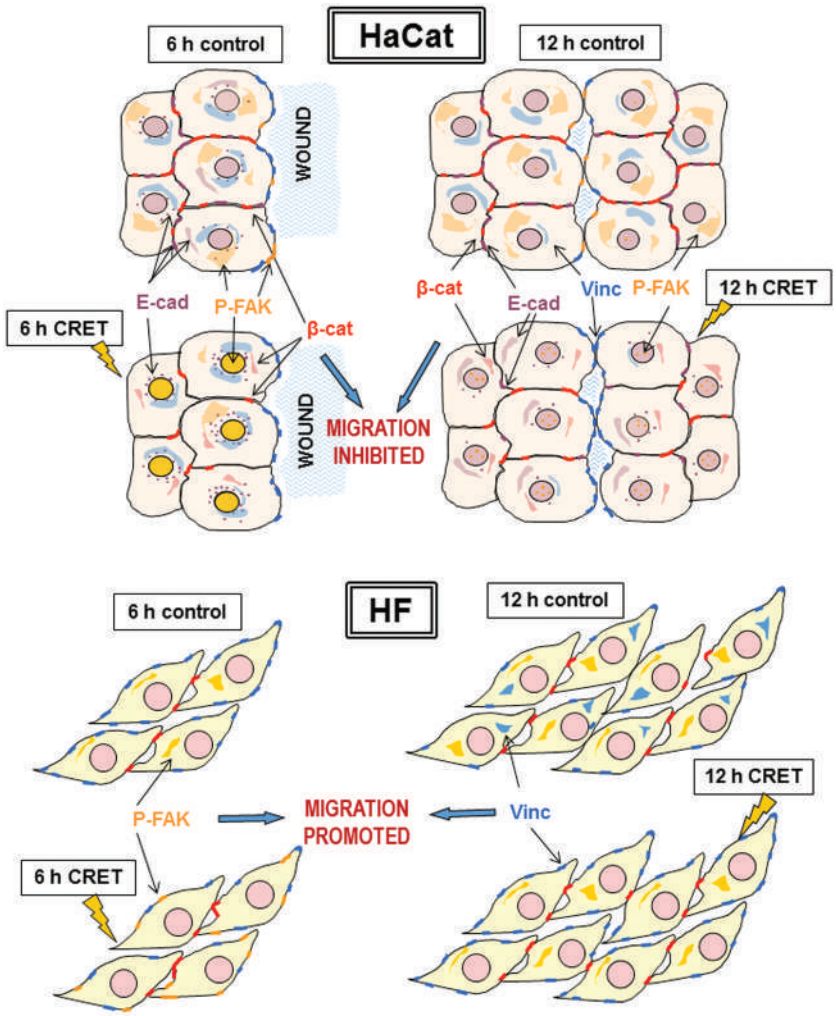


Figure 7. Protein translocation in keratinocytes (HaCaT) and fibroblasts (HF). Schematic representation of CRET-induced changes in the location of proteins involved in cell migration after 6 or 12 hours of treatment. See Discussion for detailed explanation.

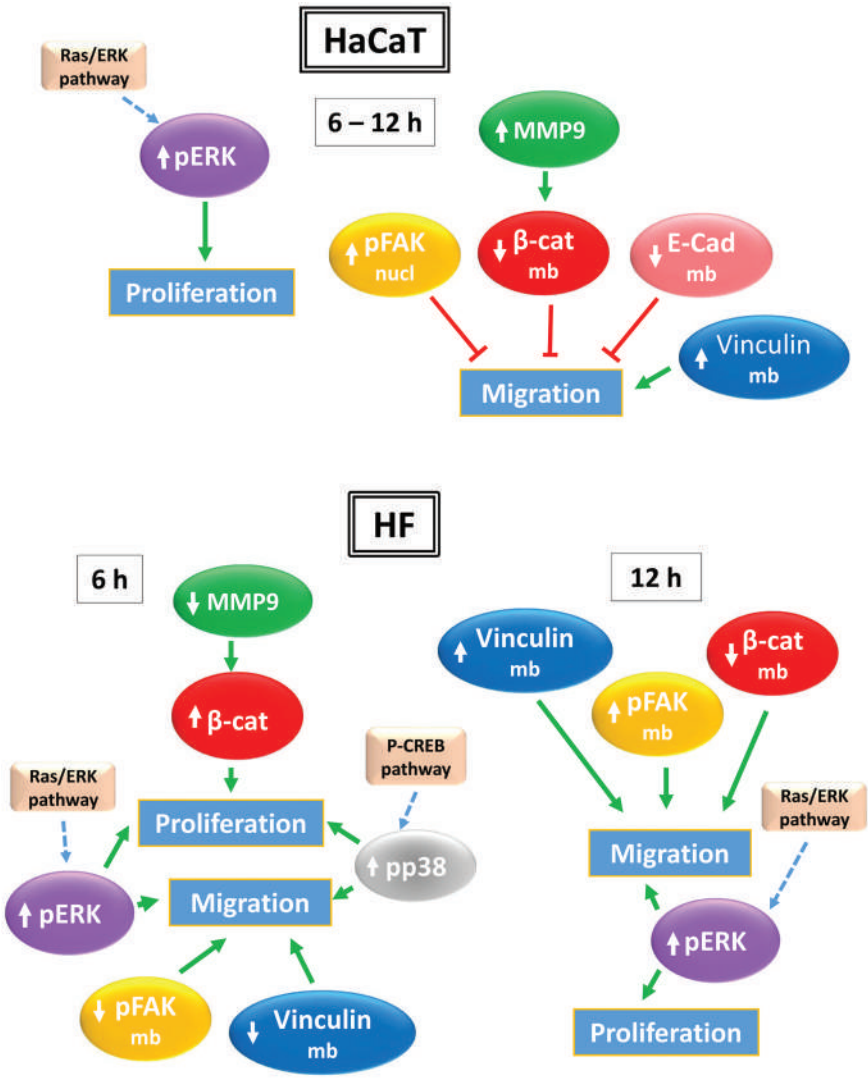


Figure 8. Protein expression in keratinocytes (HaCaT) and fibroblasts (HF). Schematic representation of CRET-induced changes in the expression of proteins involved in cell proliferation and migration after 6 or 12 hours of treatment.↑: protein overexpression; ↓: decreased expression. Green arrows: promotion. Red lines: inhibition. Dotted blue arrows: proposed pathways. See Discussion for detailed explanation.

FAK, a signaling molecule located in focal adhesion complexes, is crucial to the regulation of the integrin-mediated adhesion response. In keratinocyte cultures sham-exposed for 6 hours, the *p*-FAK labeling in cells located at the wound edge mainly appeared at the perinuclear area of the cytoplasm, as well as forming plates in the vicinity of the plasma membrane. By contrast, in the corresponding CRET-exposed samples, most of the *p*-FAK labeling was translocated to the cell nucleus (Figure 7). This type of translocation is known to be due to loss of cell-to-substrate adhesion or to inhibition of cytoplasmic *p*-FAK (Lim 2013). Thus, although immunoblotting revealed that CRET induces *p*-FAK overexpression in these cells, its nuclear location would be consistent with the inhibition of cell migration revealed by the wound closure assay. At 12 hours, *p*-FAK was located in the cytoplasmic region of the sham-exposed keratinocytes. By contrast, in CRET-exposed cells the labeling was predominantly nuclear, providing support for the evidence that the electric stimulus could inactivate the protein and block keratinocyte migration (Figures 7 and Figures 8).

In fibroblasts sham-treated for 6 hours, *p*-FAK was evenly distributed in the cytoplasm. By contrast, in CRET-treated cells the protein had moved to the immediate vicinity of the plasma membrane, a location that is typical of migrating fibroblasts (Ruest et al. 2000) and is consistent with the concomitant migratory effect revealed by the wound assay (Figure 7). In these CRET-treated samples, the immunoblot assay revealed a significant reduction in *p*-FAK expression that, like

the above described reduction in vinculin expression, could intervene in the cell-to-substrate unanchorage process (Ridley et al. 2003). After detaching, migrating cells initiate lamellipodia emission mediated by *p*-FAK overexpression (Tilghman et al. 2005), such as that displayed by fibroblasts after 12 hours of CRET exposure (Figure 8).

Intercellular adhesion is sustained by adherens junctions composed of cadherins and catenins (Mayor and Etienne-Manneville 2016). In keratinocytes, metalloproteinases (MMPs) are involved in re-epithelialization processes (Jiang et al. 2013), and cadherin cleavage by MMPs is known to promote adherent junction dissolution, favoring β-catenin internalization (Newby 2006). In the presence of the Wingless-related integration site (Wnt), internalized β-catenin is translocated to the nucleus and functions as a transcription factor for genes involved in cell migration and proliferation. In the absence of Wnt, β-catenin is phosphorylated and ubiquitinated, which induces its degradation in the proteasome and prevents migration (Tian et al. 2011). In our assays, 6 or 12 hours of CRET treatment induced MMP-9 overexpression in keratinocytes. This would lead to degradation of β-catenin-dependent intercellular junctions, which is consistent with the decreased β-catenin levels observed at 12 hours of exposure. Since in HaCaT cells treated for 6 or 12 hours the β-catenin labeling was very low in the plasma membrane and null in the nucleus, it can be assumed that β-catenin had remained in the cytoplasm, where it degraded. Such degradation would lead to blocking or slowing down migration in a fraction of the cell population (Figures 7 and Figures 8). Additionally, MMP-9 also intervenes in FAK activation at the cell membrane level, which favors cell migration through lamellipodia emission (Newby 2006). However, in the electrically treated keratinocytes FAK remained within the cell nucleus, which would have prevented its activation and inhibited cell migration.

As is typical in cells that do not establish monolayers and have few intercellular junctions, the expression of β-catenin in fibroblasts was poor and predominantly located in the vicinity of the plasma membrane. Maybe due to such a low expression, no significant changes could be detected in the location of β-catenin labeling in CRET-exposed fibroblasts. However, significant overexpression of the protein was observed in samples treated for 6 hours (Figures 7 and Figures 8). β-catenin overexpression and activation, which are involved in fibroblast proliferation and migration during wound regeneration (Poon et al. 2009) could be partly responsible for the CRET-induced proliferative response observed after 6 hours of exposure. Subsequently, after additional 6-hour treatment, a significant decrease in the expression of β-catenin, whose labeling appeared at the cell membrane level, was recorded. Such decrease could correspond to the intercellular junction degradation that precedes cell migration. This, together with the above described *p*-FAK overexpression, which promotes lamellipodia formation, could intervene in the CRET-induced migratory response revealed by the wound assay.

For proper functioning of the keratinocyte collective migration pattern, which involves coordinated movements and tensions between cells, the intercellular adhesion through adherens junctions must be maintained (Advedissian et al. 2017). Loss of E-cadherin in these junctions has been reported to inhibit protrusion formation in the cells on the migration front and to block migration (Mayor and Etienne-Manneville 2016). Our results reveal that after 6 hours of treatment, keratinocytes show decreased expression of E-cadherin and internalization of this protein from the intercellular junctions towards the cytoplasm; this effect remaining after additional 6-hour exposure (Figures 7 and Figures 8). These indications of E-cadherin inactivation at the plasma membrane level, as well as the above described effects on β-catenin, are consistent with the retarded keratinocyte migration shown by the wound assay at 6 hours of treatment. Such changes in E-cadherin expression were no longer observable at 12 hours of treatment, as cell migration had ceased once the gap closure was complete. The joint analysis of the keratinocyte response to CRET treatment indicates that the simultaneous changes induced in the expression and/or location of E-cadherin, *p*-FAK, MMP-9 and β-catenin would exert potential inhibitory effects on cell migration. These changes would be able of blocking the display of a potential migratory stimulus triggered by the above described vinculin overexpression and activation (Figure 8).

Also the MAPKs are involved in multiple cellular functions related to proliferation, differentiation, oncogenesis and stress signaling. Among these kinases, Jun N-terminal kinase (JNK), p38 and ERK play central roles in cell migration (Huang et al. 2004). Our results show that 6 hours of electric treatment induce, in both keratinocytes and fibroblasts, a *p*-ERK1/2 overexpression that could be involved in the proliferative response observed in both cell types, as well as in the migration promotion induced by CRET in fibroblasts. Also in this cell type, the 6-hour treatment induced significant *p*-p38 overexpression. This type of effect, which is capable of promoting fibroblastic migration through the *p*-CREB pathway (Nishikai-Yan Shen et al. 2017), could be involved in the described promigratory

response (Figure 8). Ongoing work extending the present study will include confirmatory analysis using specific inhibitors of proteins involved in the MAPK-ERK1/2 pathway. The potential implication of the PI3K/Akt pathway in the herein described effects on cell proliferation and migration will also be investigated.

In conclusion, the electrically induced changes in the studied proteins are consistent with the CRET effects on proliferation and migration of keratinocytes and fibroblasts, two cell types whose participation is crucial in skin repair and regeneration. Proper skin regeneration requires that formation of fibroblastic granulation tissue precedes the re-epithelialization process carried out by keratinocytes. In fact, the delayed formation of this granulation tissue is one of the main causes of complications in wound regeneration. The present results are suggestive of dual and simultaneous CRET effects in skin cells: promotion of early fibroblast migration and slowing down of keratinocyte migration. This, coupled with the CRET-induced proliferative effect in both cell types, could promote wound regeneration by stimulating granulation tissue formation, as described in wounds generated in diabetic mice and treated with RF pulses (Li et al. 2011). In this way, CRET electrostimulation could promote normotrophic wound regeneration by favoring completion of granulation tissue formation prior to closure of the outer tissue layers, thus preventing wound chronification or abnormal cicatrization.

Competing interest

The authors declare that they have no competing interests.

Funding

This work was financially supported by Fundación para la Investigación Biomédica del Hospital Ramón y Cajal, through Project FiBio-HRC No. 2015/0050.

References

Advedissian, T., V. Proux-Gillardeaux, R. Nkosi, G. Peyret, T. Nguyen, F. Poirier, M. Viguier, and F. Deshayes. 2017. E-cadherin dynamics is regulated by galectin-7 at epithelial cell surface. *Sci. Rep.* 7:17086. doi:10.1038/s41598-017-17332-y.

Barnes, R., Y. Shahin, R. Gohil, and I. Chetter. 2014. Electrical stimulation vs. standard care for chronic ulcer healing: A systematic review and meta-analysis of randomised controlled trials. *Eur. J. Clin. Invest.* 44:429–40. doi:10.1111/eci.12244.

Bito, T., Y. Tashiro, Y. Suzuki, Y. Kajiwara , H. Zeidan, M. Kawagoe, T. Sonoda, Y. Nakayama, Y. Yokota, K. Shimoura, et al. 2019. Acute effects of capacitive and resistive electric transfer (CRet) on the Achilles tendon. *Electromagn. Biol. Med* 38:48–54. doi:10.1080/15368378.2019.1567525.

Borba, G. C., B. Hochman, R. E. Liebano, M. Enokihara, and L. M. Ferreira. 2011. Does preoperative electrical stimulation of the skin alter the healing process? *J. Surg. Res.* 166:324–29. doi:10.1016/j.jss.2009.08.018.

Conner-Kerr, T., and R. A. Isenberg. 2012. Retrospective analysis of pulsed radiofrequency energy therapy use in the treatment of chronic pressure ulcers. *Adv Skin Wound Care* 25:253–60. doi:10.1097/01.ASW.0000415342.37554.ed.

Fletcher, S. 2011. Successful treatment of venous stasis ulcers with combination compression therapy and pulsed radio frequency energy in a patient scheduled for amputation. *J. Wound. Ostomy. Continence. Nurs* 38:91–94. doi:10.1097/WON.0b013e318202b4b1.

Frykberg, R., E. Martin, A. Tallis, and E. Tierney. 2011. A case history of multimodal therapy in healing a complicated diabetic foot wound: Negative pressure, dermal replacement and pulsed radio frequency energy therapies. *Int. Wound. J* 8:132–39. doi:10.1111/j.1742-481X.2010.00759.x.

Goldmann, W. H. 2016. Role of vinculin in cellular mechanotransduction. *Cell Biol. Int.* 40:241–56. doi:10.1002/cbin.10563.

Grimnes, S., and Ø. G. Martinsen. 2000. *Bioimpedance and Bioelectricity Basics*, 71–73. London: Academic Press. Harcourt and Technology Co.

Han, G., and R. Ceilley. 2017. Chronic Wound Healing: A Review of Current Management and Treatments. *Adv. Ther.* 34:599–610. doi:10.1007/s12325-017-0478-y.

Hernandez-Bule, M. L., C. L. Paino, M. A. Trillo, and A. Ubeda. 2014a. Electric stimulation at 448 kHz promotes proliferation of human mesenchymal stem cells. *Cell. Physiol. Biochem* 34:1741–55. doi:10.1159/000366375.

Hernandez-Bule, M. L., J. Martinez-Botas, M. A. Trillo, C. L. Paíno, and A. Úbeda. 2016. Antiadipogenic effects of subthermal electric stimulation at 448 kHz on differentiating human mesenchymal stem cells. *Mol. Med. Rep.* 13:3895–903. doi:10.3892/mmr.2016.5032.

Hernandez-Bule, M. L., M. A. Trillo, and A. Ubeda. 2014b. Molecular mechanisms underlying antiproliferative and differentiating responses of hepatocarcinoma cells to subthermal electric stimulation. *PLoS One* 8:e84636. doi:10.1371/journal.pone.0084636.eCollection.

Hernandez-Bule, M. L., M. A. Trillo, M. A. Cid, J. Leal, and A. Ubeda. 2007. In vitro exposure to 0.57-MHz electric currents exerts cytostatic effects in HepG2 human hepatocarcinoma cells. *Int. J. Oncol.* 30:583–92.

Hernandez-Bule, M. L., M. A. Trillo, M. A. Martinez-Garcia, C. Abilahoud, and A. Ubeda. 2017. Chondrogenic differentiation of adipose-derived stem cells by radiofrequency electric stimulation. *J. Stem. Cell. Res. Ther* 7. doi:10.4172/2157-7633.1000407.

Houghton, P. E., K. E. Campbell, C. H. Fraser, C. Harris, D. H. Keast, P. J. Potter, K. C. Hayes, and M. G. Woodbury. 2010. Electrical stimulation therapy increases rate of healing of pressure ulcers in community-dwelling people with spinal cord injury. *Arch. Phys. Med. Rehabil.* 91:669–78. doi:10.1016/j.apmr.2009.12.026.

Huang, C., K. Jacobson, and M. D. Schaller. 2004. MAP kinases and cell migration. *J. Cell. Sci* 117:4619–28. doi:10.1242/jcs.01481.

Jiang, X. P., D. X. Zhang, M. Teng, Q. Zhang, J. P. Zhang, and Y. S. Huang. 2013. Downregulation of CD9 in keratinocyte contributes to cell migration via upregulation of matrix metalloproteinase-9. *PLoS One* 8:e77806. doi:10.1371/journal.pone.0077806.eCollection2013.

Kanji, S., and H. Das. 2017. Advances of stem cell therapeutics in cutaneous Wound healing and regeneration. *Mediators. Inflamm.* (2017:5217967. doi:10.1155/2017/5217967.

Kao, H. K., Q. Li, B. Flynn, X. Qiao, J. W. Ruberti, G. F. Murphy, and L. Guo. 2013. Collagen synthesis modulated in wounds treated by pulsed radiofrequency energy. *Plast. Reconstr. Surg* 131:490e–8e. doi:10.1097/PRS.0b013e3182827636.

Kotnik, T., and D. Miklavcic. 2000. Theoretical evaluation of distributed power dissipation in biological cells exposed to electric fields. *Bioelectromagnetics* 21:385–94. doi:10.1002/1521-186X(200007)21:5<385::AID-BEM7>3.0.CO;2-F.

Kumaran, B., and T. Watson. 2019. Treatment using 448 kHz capacitive resistive monopolar radiofrequency improves pain and function in patients with osteoarthritis of the knee joint: A randomised controlled trial. *Physiotherapy* 105:98–107. doi:10.1016/j.physio.2018.07.004.

Lala, D., S. J. Spaulding, S. M. Burke, and P. E. Houghton. 2016. Electrical stimulation therapy for the treatment of pressure ulcers in individuals with spinal cord injury: A systematic review and meta-analysis. *Int. Wound. J* 13:1214–26. doi:10.1111/iwj.12446.

Li, L., R. Hartley, B. Reiss, Y. Sun, J. Pu, D. Wu, F. Lin, T. Hoang, S. Yamada, J. Jiang, and M. Zhao. 2012. E-cadherin plays an essential role in collective directional migration of large epithelial sheets. *Cell. Mol. Life. Sci* 69. 2012:2779–89. doi:10.1007/s00018-012-0951-3.

Li, Q., H. Kao, E. Matros, C. Peng, G. F. Murphy, L. Guo. 2011. Pulsed radiofrequency energy accelerates wound healing in diabetic mice. *Plast. Reconstr. Surg* 127:2255–62. doi:10.1097/PRS.0b013e3182131bb5.

Lim, S. T. 2013. Nuclear FAK: A new mode of gene regulation from cellular adhesions. *Mol. Cells.* 36:1–6. doi:10.1007/s10059-013-0139-1.

Mathworks. Image processing toolbox. Accessed 2020 March 12. http://es.mathworks.com/products/image/

Mayor, R., and S. Etienne-Manneville. 2016. The front and rear of collective cell migration. *Nat. Rev. Mol. Cell. Biol* 17:97–109. doi:10.1038/nrm.2015.14.

Meyer, P. F., P. de Oliveira, F. K. B. A. Silva, A. C. S. da Costa, C. R. A. Pereira, S. Casenave, R. M. V. Silva, L. G. Araújo-Neto, S. D. Santos-Filho, E. Aizamaque, et al. 2017. Radiofrequency treatment induces fibroblast growth factor 2 expression and subsequently promotes neocollagenesis and neoangiogenesis in the skin tissue. *Lasers. Med. Sci* 32:1727–36. doi:10.1007/s10103-017-2238-2.

Naranjo, P., J. L. López-Estebaranz, T. Shoaib. 2020. Non-ablative capacitive resistive 448 kHz radiofrequency for wrinkle reduction pilot study. *Aesthetic. Medicine* 6/N.2:41–48.

Newby, A. C. 2006. Matrix metalloproteinases regulate migration, proliferation, and death of vascular smooth muscle cells by degrading matrix and non-matrix substrates. *Cardiovasc. Res* 69:614–24. doi:10.1016/j.cardiores.2005.08.002.

Nishikai-Yan Shen, T., S. Kanazawa, M. Kado, K. Okada, L. Luo, A. Hayashi, H. Mizuno, and R. Tanaka. 2017. Interleukin-6 stimulates Akt and p38 MAPK phosphorylation and fibroblast migration in non-diabetic but not diabetic mice. *PLoS One* 12:e0178232. doi:10.1371/journal.pone.0178232.eCollection2017.

Poon, R., S. A. Nik, J. Ahn, L. Slade, and B. A. Alman. 2009. Beta-catenin and transforming growth factor beta have distinct roles regulating fibroblast cell motility and the induction of collagen lattice contraction. *BMC. Cell. Biol* 10:38. doi:10.1186/1471-2121-10-38.

Ridley, A. J., M. A. Schwartz, K. Burridge, R. A. Firtel, M. H. Ginsberg, G. Borisy, J. T. Parsons, and A. R. Horwitz. 2003. Cell migration: Integrating signals from front to back. *Science* 302:1704–09. doi:10.1126/science.1092053.

Rouabhia, M., H. Park, S. Meng, H. Derbali, and Z. Zhang. 2013. Electrical stimulation promotes wound healing by enhancing dermal fibroblast activity and promoting myofibroblast transdifferentiation. *PLoS One* 19:e71660. doi:10.1371/journal.pone.0071660.eCollection2013.

Ruest, P. J., S. Roy, E. Shi, R. L. Mernaugh, and S. K. Hanks. 2000. Phosphospecific antibodies reveal focal adhesion kinase activation loop phosphorylation in nascent and mature focal adhesions and requirement for the autophosphorylation site. *Cell. Growth. Differ* 11:41–48.

Santoro, M. M., and G. Gaudino. 2005. Cellular and molecular facets of keratinocyte reepithelization during wound healing. *Exp. Cell. Res* 304:274–86. doi:10.1016/j.yexcr.2004.10.033.

Stadelmann, W. K., A. G. Digenis, and G. R. Tobin. 1998. Physiology and healing dynamics of chronic cutaneous wounds. *Am. J. Surg.* 176:26S–38S. doi:10.1016/S0002-9610(98)00183-4.

Tai, G., M. Tai, and M. Zhao. 2018. Electrically stimulated cell migration and its contribution to wound healing. *Burns Trauma* 9:20. doi:10.1186/s41038-018-0123-2.eCollection 2018.

Takahashi, K., S. Hirabayashi, S. Hirabayashi, N. Tsuzuki, and L. Zhong-Shiet. 1999. Clinical effects of capacitive electric transfer hyperthermia for lumbago. *J. Phys. Ther. Sci* 11:45–51. doi:10.1589/jpts.11.45.

Thievessen, I., N. Fakhri, J. Steinwachs, V. Kraus, R. S. McIsaac, L. Gao, B-C. Chen, M. A. Baird, M. W. Davidson, E. Betzig, et al. 2015. Vinculin is required for cell polarization, migration, and extracellular matrix remodeling in 3D collagen. *FASEB J.* 29:4555–67. doi:10.1096/fj.14-268235.

Tian, X., Z. Liu, B. Niu, J. Zhang, T. K. Tan, S. R. Lee, Y. Zhao, D. C. H. Harris, and G. Zheng. 2011. E-cadherin/β-catenin complex and the epithelial barrier. *J. Biomed. Biotechnol.* (2011:567305. doi:10.1155/2011/567305.

Tilghman, R. W., J. K. Slack-Davis, N. Sergina, K. H. Martin, M. Iwanicki, E. D. Hershey, H. E. Beggs, L. F. Reichardt, and J. T. Parsons. 2005. Focal adhesion kinase is required for the spatial organization of the leading edge in migrating cells. *J. Cell. Sci* 118:2613–23. doi:10.1242/jcs.02380.